

Influence of Spin Wave Excitations on the Ferromagnetic Phase Diagram in the Hubbard-Model

W. Rumsch* and W. Nolting

Lehrstuhl Festkörpertheorie

Institut für Physik

Invalidenstrasse 110

D-10115 Berlin

Humboldt-Universität zu Berlin

Mathematisch-Naturwissenschaftliche Fakultät I

(Dated: November 8, 2018)

The subject of the present paper is the theoretical description of collective electronic excitations, i.e. spin waves, in the Hubbard-model. Starting with the widely used Random-Phase-Approximation, which combines Hartree-Fock theory with the summation of the two-particle ladder, we extend the theory to a more sophisticated single particle approximation, namely the Spectral-Density-Ansatz. Doing so we have to introduce a ‘screened’ Coulomb-interaction rather than the bare Hubbard-interaction in order to obtain physically reasonable spinwave dispersions. The discussion following the technical procedure shows that comparison of standard RPA with our new approximation reduces the occurrence of a ferromagnetic phase further with respect to the phase-diagrams delivered by the single particle theories.

PACS numbers: (71.10.Fd,75.10.Lp,75.30.Ds,75.40.Gb)

I. INTRODUCTION

Recent publications^{1,2,3,4,5,6,7,8} on the theoretical description of spin waves in the Hubbard-model demonstrate an increased interest in the subject. The Hubbard-model, originally introduced in 1963 by Hubbard and others^{9,10,11}, is one of the best investigated models in many-body-theory. It is commonly accepted to be the simplest model to hold for the itinerant as well as the localized character of the valence electrons in partially filled 3d-shells of transition and rare earth metals such as Ni, Fe, Co. Despite the continuing interest only a handful of exact statements can be given on the possibility of a ferromagnetic groundstate.

Actually the model appears not to be very convenient for ferromagnetism. The exact solution of the $1 - D$ Hubbard-model¹² suggests the ground-state to be an antiferromagnetic one as well as the fact that in all dimensions the half-filled Hubbard-model can be mapped onto the antiferromagnetic Heisenberg-model in the strong coupling regime $\frac{U}{W} > 1$, where W denotes the bandwidth and U the interaction strength. Furthermore the Mermin-Wagner-Theorem¹³ forbids the existence of magnetic long range order for $D < 3$ at finite temperature T . The zero-bandwidth limit excludes a ferromagnetic solution because $n_\uparrow = n_\downarrow$ is always valid¹⁴, herein n_σ is the occupation number of $\uparrow(\downarrow)$ -spin.

If at all, we expect a ferromagnetic phase to occur in the strong coupling regime $\frac{U}{W} > 1$, away from exact half-filling in $D = 3$.

The simple Hartree-Fock Approximation (HF) is able to deliver a ferromagnetic ground state in the Hubbard-model as long as the interaction strength is sufficiently large or respectively the density of states at the Fermi-surface $\rho_0(\epsilon_F)$ is considerably high, manifested in the fa-

mous Stoner-criterion $1 \leq U\rho_0(\epsilon_F)$.

It is a well known fact that HF-theory overestimates the existence of spontaneous ferromagnetism. In particular the Curie-temperatures are orders of magnitude too high but nevertheless HF points in the right direction.

A more sophisticated approach beside others is the Spectral-Density-Ansatz (SDA)¹⁵ based on Harris’s and Lange’s¹⁶ statements who have shown that the spectral density is dominated by two strongly developed peaks at the centre of the band T_0 and at $T_0 + U$ when a finite hopping probability is taken into account. SDA basically is a two-pole ansatz of the form $S_{\mathbf{k}\sigma}(E - \mu) = \hbar \sum_{i=1,2} \alpha_{i\sigma}(\mathbf{k}) \delta(E - E_{i\sigma}(\mathbf{k}))$, where the in the first place unknown parameters, spectral weights $\alpha_{i\sigma}$ and peak positions $E_{i\sigma}(\mathbf{k})$, are fitted via the exactly calculable spectral moments¹⁵. The SDA-approximation results in a much more reliable phase-diagram and more trustworthy Curie-temperatures than HF-approximation. In a single particle theory, however, collective excitations are not present. The study of these excitations in itinerant ferromagnets requires the examination of the transversal magnetic susceptibility. Collective excitations have a strong influence on the stability of the ferromagnetic phase in particular at higher temperatures since the excitations of magnons tend to destroy the magnetic ordering. This is the reason for our interest in describing collective excitations in the Hubbard-model.

Facing the complexity of the many-body problem one usually has to apply one or more suitable and reasonable approximations in order to find physically interpretable results. Certain sequences of such approximations will be presented in the following sections. In Sect. II we will develop the theory for the magnetic susceptibility which results in the Random-Phase-Approximation (RPA). RPA combines ladder-approximation of the two-particle Green

function with the HF-approximation of the one-particle Green function and is discussed in more detail in Sect. III.

In Sect. IV we will combine ladder-approximation of the two-particle Green function with the more sophisticated SDA-approach of the one particle Green function which makes a further approximation necessary, namely a screened interaction V_{eff} , but will result in physically reasonable behaviour of the collective mode. This is a new approach to the at the beginning mentioned spin wave problem and discussed in detail. We present our results in Sect. V and discuss them with respect to results of different authors and will finally close with a short summary and an outlook in Sect. VI.

II. THEORY

A. Transversal Magnetic Susceptibility

We use the so-called one band Hubbard-Hamiltonian where orbital degrees of freedom are neglected for simplicity. It reads in second quantized form in Fourier-space as

$$\hat{H} = \sum_{\mathbf{k}\sigma} (\epsilon(\mathbf{k}) - \mu) a_{\mathbf{k}\sigma}^+ a_{\mathbf{k}\sigma} + \frac{1}{2} \frac{U}{N} \sum_{\mathbf{k}\mathbf{p}\mathbf{q}\sigma} a_{\mathbf{k}\sigma}^+ a_{\mathbf{k}+\mathbf{q}\sigma}^+ a_{\mathbf{p}-\sigma}^+ a_{\mathbf{p}-\mathbf{q}-\sigma}. \quad (1)$$

The operators $a_{\mathbf{k}\sigma}^+$ ($a_{\mathbf{k}\sigma}$) in (1) are the creation (annihilation) operators for fermions in \mathbf{k} -space.

Spin waves are collective excitations of the solid's state electronic system. The group of conduction electrons take on a coherent quantum state which is described as a gapless excitation with energy $E = \hbar\omega(\mathbf{q})$, where \mathbf{q} is the wavevector of a so-called spinwave. The spin wave dispersion usually behaves as $E_{\mathbf{q}} \simeq D\mathbf{q}^2$ for small \mathbf{q} -values, where D is the stiffness constant.

In order to describe the excited system we make use of the retarded polarisation propagator and will analyze it with help of a diagrammatic technique. In our case the polarisation propagator is the transversal magnetic susceptibility. It is a two-particle Green function and given in energy representation by

$$\chi_{ij}^{+-}(E) = -\frac{1}{\hbar^2} \langle \langle S_i^+; S_j^- \rangle \rangle_E \quad (2)$$

where the spin-operators are

$$S_i^+ = \hbar a_{i\uparrow}^+ a_{i\downarrow} \quad (3)$$

$$S_j^- = \hbar a_{j\downarrow}^+ a_{j\uparrow}. \quad (4)$$

Within Matsubara formalism^{14,17}, which is a generalisation of the Green function formalism to the imaginary

time scale, this two-particle quantity is given by

$$\begin{aligned} -\chi_q^{+-}(E_n) &= \frac{1}{N} \sum_{\mathbf{k}\mathbf{p}} \int_0^{\hbar\beta} d\tau \exp\left(\frac{i}{\hbar} E_n \tau\right) \times \\ &\quad \langle T_{\tau} [a_{\mathbf{k}\uparrow}^+(\tau) a_{\mathbf{k}+\mathbf{q}\downarrow}(\tau) a_{\mathbf{p}\downarrow}^+(0) a_{\mathbf{p}-\mathbf{q}\uparrow}(0)] \rangle \\ &= \hat{\chi}_q^{+-}(E_n) \end{aligned} \quad (5)$$

The time-ordering operator T_{τ} in (5), for which a generalized Wick's theorem exists¹⁴, sorts operators in a product of operators by their time-arguments. Matsubara-frequencies, denoted by subscript n , are given by

$$E_n = \begin{cases} 2n \frac{\pi}{\beta} & : \text{bosons} \\ (2n+1) \frac{\pi}{\beta} & : \text{fermions} \end{cases}. \quad (6)$$

One obtains the retarded form of (5), the actual interesting quantity, simply by analytical continuation. The poles of (5) yield the spin wave excitation spectrum. Diagrammatically (5) is represented by the graph given on the left side of Fig. 1. The representation with help of the vertex part (shaded triangle on the right of Fig. 1) is very handy because it allows an approximate partial summation. The vertex part plays a similar role as the selfenergy

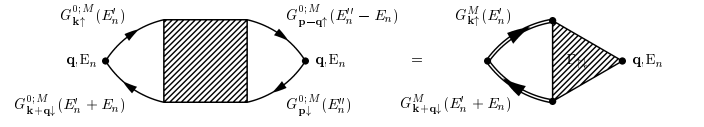


FIG. 1: Representation of the polarisation propagator with help of the vertex function

in a single particle theory. The doubly lined propagators on the right side of Fig. 1 indicate that we have to use the full single particle Green function $G_{\mathbf{k}\sigma}^M(E_n)$ instead of the free Green function $G_{\mathbf{k}\sigma}^{0;M}(E_n)$ indicated by singly lined propagators as on the left side of Fig. 1.

For the vertex part we have to find a practicable and physically reasonable approximation. Summing up the ladder graphs (see Fig. 2) we find with help of the

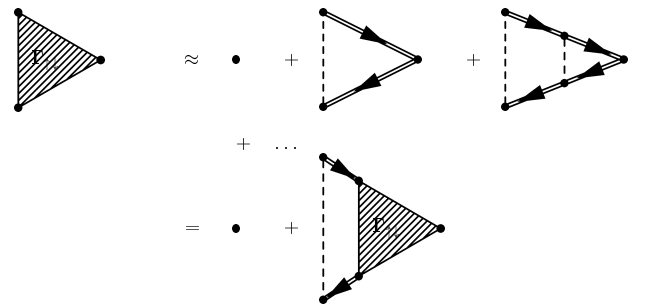


FIG. 2: Partial summation of the ladder graphs

diagram-'dictionary'¹⁴

$$\Gamma_{\uparrow\downarrow}(\mathbf{q}, E_n; \mathbf{k}, E'_n) = 1 + \frac{-1}{\hbar^2\beta} \frac{U}{N} \sum_{\mathbf{p}} \sum_{E''_n} G_{\mathbf{p}\downarrow}^M(E''_n - E_n) G_{\mathbf{p}\uparrow}^M(E''_n) \Gamma_{\uparrow\downarrow}(\mathbf{q}, E_n; \mathbf{p}, E''_n). \quad (7)$$

The coupling parameter U in the Hubbard-model is a constant which is why we can write

$$\Gamma_{\uparrow\downarrow}(\mathbf{q}, E_n; \mathbf{k}, E'_n) = \Gamma_{\uparrow\downarrow}(\mathbf{q}, E_n; \mathbf{p}, E''_n) \equiv \Gamma(\mathbf{q}, E_n) \quad (8)$$

for the vertex part.

Introducing

$$\Lambda_{\uparrow\downarrow}(\mathbf{q}, E_n) = -\frac{1}{\hbar^2\beta} \frac{1}{N} \sum_{\mathbf{k}} \sum_{E'_n} G_{\mathbf{k}\uparrow}^M(E'_n) G_{\mathbf{k}+\mathbf{q}\downarrow}^M(E_n + E'_n) \quad (9)$$

we write for the whole propagator:

$$\hat{\chi}_{\mathbf{q}}^{+-}(E_n) = \frac{\hbar \cdot \Lambda_{\uparrow\downarrow}(\mathbf{q}, E_n)}{1 - U \cdot \Lambda_{\uparrow\downarrow}(\mathbf{q}, E_n)}. \quad (10)$$

The abbreviation $\Lambda_{\uparrow\downarrow}(\mathbf{q}, E_n)$ on the right side of (10) represents the polarisation propagator of zeroth order or pair bubble where no interaction line connects two vertex points.

Now, finding (9) solves the problem. This task can be fulfilled by first rewriting (9) with help of the spectral representation of the Matsubara function, i.e. we use

$$G_{\mathbf{k}\uparrow}^M(E'_n) = \int_{-\infty}^{\infty} dE_1 \frac{S_{\mathbf{k}\uparrow}(E_1)}{iE'_n - E_1} \quad (11)$$

$$G_{\mathbf{k}+\mathbf{q}\downarrow}^M(E'_n + E_n) = \int_{-\infty}^{\infty} dE_2 \frac{S_{\mathbf{k}+\mathbf{q}\downarrow}(E_2)}{i(E'_n + E_n) - E_2}.$$

and write for $\Lambda_{\uparrow\downarrow}(\mathbf{q}, E_n)$:

$$\Lambda_{\uparrow\downarrow}(\mathbf{q}, E_n) = \frac{-1}{\hbar^2\beta} \frac{1}{N} \sum_{\mathbf{k}} \sum_{E'_n} \int_{-\infty}^{\infty} dE_1 \int_{-\infty}^{\infty} dE_2 \times \frac{S_{\mathbf{k}\uparrow}(E_1)}{iE'_n - E_1} \cdot \frac{S_{\mathbf{k}+\mathbf{q}\downarrow}(E_2)}{i(E'_n + E_n) - E_2}. \quad (12)$$

For technical reasons we introduce two other abbreviations namely,

$$F(E_n; E_1, E_2) = -\frac{1}{\hbar^2\beta} \sum_{E'_n} \frac{1}{iE'_n - E_1} \times \frac{1}{i(E'_n + E_n) - E_2} \quad (13)$$

and

$$K_{\mathbf{q}}(E_1, E_2) = \frac{1}{N} \sum_{\mathbf{k}} S_{\mathbf{k}\uparrow}(E_1) S_{\mathbf{k}+\mathbf{q}\downarrow}(E_2). \quad (14)$$

The polarisation propagator then becomes $\Lambda_{\uparrow\downarrow}(\mathbf{q}, E_n) = \int_{-\infty}^{\infty} dE_1 dE_2 F(E_n; E_1, E_2) \cdot K_{\mathbf{q}}(E_1, E_2)$. Both expression (13) und (14) can be treated independently.

Evaluation of (13) requires the sum over Matsubara frequencies¹⁴ which results in

$$F(E_n; E_1, E_2) = \frac{1}{\hbar^2} \left[\frac{\tilde{f}_-(E_2) - \tilde{f}_-(E_1)}{iE_n - (E_2 - E_1)} \right] \quad (15)$$

$$\text{where } \tilde{f}_-(E_{1,2}) = \frac{1}{e^{\beta(E_{1,2})} + 1}.$$

The polarisation propagator $\Lambda_{\uparrow\downarrow}(\mathbf{q}, E_n)$ now looks with $\tilde{E}_{1,2} \rightarrow (E_{1,2} - \mu)$ like

$$\Lambda_{\uparrow\downarrow}(\mathbf{q}, E_n) = \frac{1}{N\hbar^2} \sum_{\mathbf{k}} \int_{-\infty}^{+\infty} dE_1 dE_2 \frac{[f_-(\tilde{E}_2) - f_-(\tilde{E}_1)]}{iE_n - (E_2 - E_1)} \times S_{\mathbf{k}\uparrow}(\tilde{E}_1) \cdot S_{\mathbf{k}+\mathbf{q}\downarrow}(\tilde{E}_2). \quad (16)$$

Here $f_-(\tilde{E}_{1,2})$ in the numerator is the Fermi function.

In order to represent the transversal susceptibility (5) as a functional of a product of two single particle spectral densities we performed a ladder approximation which delivereded the desired form (16). Up to now we did not make any statement about the one-particle spectral densities in (16). On account of the complexity of the many-body problem we have to apply a suitable approximation for the single particle spectral densities in (16). In the following section we will do exactly this with the HF-approximation.

III. RANDOM-PHASE-APPROXIMATION

Evaluation of (16) requires a three-dimensional summation over wavevectors \mathbf{k} and $\mathbf{k} + \mathbf{q}$ respectively.

The energy-dispersion for the conduction band in Tight-Binding-Approximation is given for the *bcc*-lattice by

$$\epsilon(\mathbf{k})^{bcc} = Z_1 T_1 \cos(k_x a) \cos(k_y a) \cos(k_z a) + T_0 \quad (17)$$

and for the *fcc*-lattice by

$$\epsilon(\mathbf{k})^{fcc} = 4Z_1 T_1 [\cos(\frac{1}{2}k_x a) \cos(\frac{1}{2}k_y a) + \cos(\frac{1}{2}k_y a) \cos(\frac{1}{2}k_z a) + \cos(\frac{1}{2}k_z a) \cos(\frac{1}{2}k_x a)] + T_0. \quad (18)$$

The Hopping-integral T_1 for next nearest neighbours is given by $T_1 = -\frac{W}{2Z_1}$, where we used a bandwidth of $W = 1\text{eV}$ for all numerical calculations, Z_1 denotes the number of next nearest neighbours ($Z_1^{bcc} = 8$ and $Z_1^{fcc} = 12$), the center of the Band was choosen to be $T_0 = 0$. In order to reduce the numerical effort to a minimum we use a

similar \mathbf{q} -separation procedure as given in²⁴ where the remaining \mathbf{k} -summation can be transformed into a one-dimensional energy-integration. This is due to the fact that the expression

$$\frac{1}{N} F(\epsilon(\mathbf{k})) = \int F(x) \rho^{BDOS}(x) \quad (19)$$

where

$$\rho^{BDOS}(x) \frac{1}{N} \sum_{\mathbf{k}} \delta(x - \epsilon(\mathbf{k})) \quad (20)$$

is true for any \mathbf{k} -dependent function whose \mathbf{k} -dependence is only given by a $\epsilon(\mathbf{k})$ -dependence.

This procedure allows us to apply the numerical formulas given by Jelitto¹⁸ for the Bloch density of states (BDOS). Picture 3 shows the BDOS for the fcc and bcc lattice resulting from these formulas.

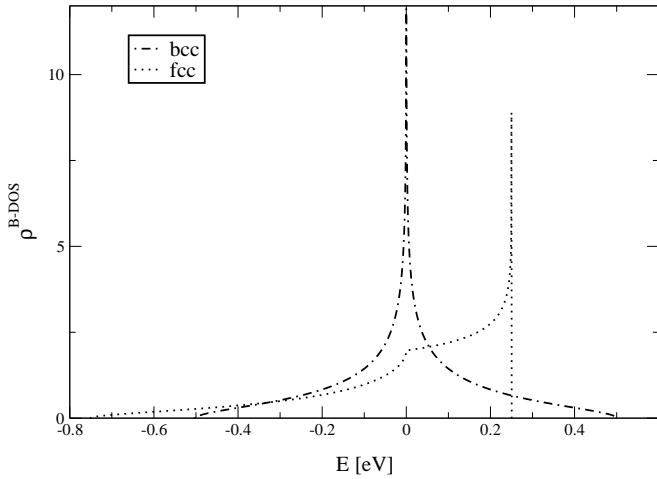


FIG. 3: Bloch Density of States, bandwidth $W = 1\text{eV}$, center of the band $T_0 = 0$

For the situation where $\mathbf{q} = \mathbf{0}$, however, the \mathbf{q} -separation is not needed and one easily can check if there exists a gapless excitation with $\omega(\mathbf{q}) \rightarrow 0$ as proposed by Lange²¹. Useful is the following representation of the HF-spectral density

$$S_{\mathbf{k}\sigma}(E) = \hbar\delta(E - \epsilon(\mathbf{k}) - U\langle n_{-\sigma} \rangle + \mu). \quad (21)$$

The propagator (16) reduces with (21) and $E_{\mathbf{k},\sigma} = \epsilon_{\mathbf{k}} + U\langle n_{\sigma} \rangle$ to

$$\Lambda_{\uparrow\downarrow}(\mathbf{q}, E_n) = \frac{1}{N} \sum_{\mathbf{k}} \frac{f_{-}(E_{\mathbf{k}+\mathbf{q},\uparrow}) - f_{-}(E_{\mathbf{k},\downarrow})}{iE_n - (E_{\mathbf{k}+\mathbf{q},\uparrow} - E_{\mathbf{k},\downarrow})}. \quad (22)$$

For $\mathbf{q} = \mathbf{0}$ one easily can perform the summation over wave vectors because

$$\langle n_{\sigma} \rangle = \frac{1}{N} \sum_{\mathbf{k}} f_{-}(E_{\mathbf{k},\sigma}) = \frac{1}{N} \sum_{\mathbf{k}} \langle n_{\sigma}(\mathbf{k}) \rangle. \quad (23)$$

The condition for the denominator of (10) to be zero is

$$1 - U \cdot \text{Re}\Lambda_{\uparrow\downarrow}(\mathbf{q} = \mathbf{0}, E) = 0 \quad (24)$$

or equivalently

$$1 - \frac{-U \cdot 2m}{E - U \cdot 2m + i0^{+}} = 0 \quad (25)$$

Here $m = \frac{1}{2}(n_{\uparrow} - n_{\downarrow})$ denotes the magnetisation. One immediately sees that this condition is fulfilled only for $E \equiv 0$ which means that using HF-theory a well defined gapless excitation exists.

Edwards²⁰ already stated that excited states with one reversed spin in bandferromagnets must have an energy of the form $E \sim \epsilon(\mathbf{k}') - \epsilon(\mathbf{k}) + J$ where J is a \mathbf{k} -independent constant that contains the correlation energy. Clearly in HF-theory this is the case. In the event of transitions between majority- and minority-spin band the excitation energy is given by $\Delta E_{\uparrow\downarrow}(\mathbf{k}; \mathbf{q}) = \epsilon(\mathbf{k} + \mathbf{q}) - \epsilon(\mathbf{k}) + \Delta E_{ex}$, where $\Delta E_{ex} = 2mU$ is the rigid exchange splitting energy of the HF-theory.

IV. MODIFIED RANDOM PHASE APPROXIMATION

In this section we will use the SDA-theory as the single particle input for the two particle propagator (16). Compared to HF-approximation SDA is a real many-body theory able to deliver ferromagnetism in the Hubbard-model and tested by means of comparison to different advanced many-body theories concerning ferromagnetism in the Hubbard-model. Comparison of SDA, Modified-Alloy-Analogy (MAA) and Modified-Perturbation-Theorie with the numerical exact Quantum-Monte-Carlo-Simulation²⁸ indicates that the qualitative behaviour of the SDA phase-diagram is correctly displayed. Furthermore are the Curie-temperatures orders of magnitude lower than in HF-theory and therefore much more reliable. HF-theory overestimates the occurrence of ferromagnetism in the Hubbard-model, although the tendency is right, in a incredulous manner.

Though one cannot simply check the validity of the theory by putting the SDA-selfenergy (or equivalently the spectral density) for $\mathbf{q} = \mathbf{0}$ into the expression (16) because the selfenergy in SDA consists of a Stoner or HF-like part and a spin dependent rest. This spin-dependence prevents us from being able to check the validity in a similar manner as with HF-theory.

$$\Sigma_{\mathbf{k}\sigma}^{SDA}(E) = Un_{-\sigma} + \frac{U^2 n_{-\sigma} (1 - n_{-\sigma})}{E - B_{-\sigma} - U(1 - n_{-\sigma})}. \quad (26)$$

The spin dependence of the second term of (26) is mainly given by the so called band shift $B_{-\sigma}$. This spin-dependence in SDA-theory is the main improvement and

leads to a shift of \uparrow - and \downarrow -quasiparticle-density of states (QDOS), for further details on the SDA see²⁴.

However, the similarity of (26) to the Stoner self energy let us hope that connecting SDA with ladder approximation could work out and might even hold an improvement. But numerical evaluation of (16) using SDA-theory as input in form of a sum of weighted δ -functions shows negative excitation energies which are unphysical.

With no apparent reason both approximations, the ladder approximation for the two-particle propagator and the SDA for the single particle propagator are not fully compatible.

The idea now was to introduce an effective Coulomb interaction V_{eff} in order to replace the Hubbard- U in (10) and hopefully be able to shift the negative excitation energies to the right energetic position. This was done numerically via the condition

$$V_{eff} = \begin{cases} U & : \text{if } \text{Re} \Lambda_{\uparrow\downarrow}(\mathbf{q} = \mathbf{0}, E = 0) = \frac{1}{U} \\ \text{Re} \frac{1}{\Lambda_{\uparrow\downarrow}(\mathbf{0}, 0)} & : \text{else} \end{cases},$$

Indeed, replacing the Hubbard- U in the polarisation propagator (10) with V_{eff} given by the above condition the unphysical behaviour could be repaired. The susceptibility (10) now is to look at as

$$\hat{\chi}_{\mathbf{q}}^{+-(\text{MRPA})}(E_n) = \frac{\hbar \cdot \Lambda_{\uparrow\downarrow}^{(\text{SDA})}(\mathbf{q}, E_n, U)}{1 - V_{eff} \cdot \Lambda_{\uparrow\downarrow}^{(\text{SDA})}(\mathbf{q}, E_n, U)}. \quad (27)$$

The term $\Lambda^{(\text{SDA})}$ in (27) is (16) with the appropriate input of the SDA-single particle density of states.

The introduction of the effective or screened interaction of course is to rate as yet another approximation. But the interaction in a two particle theory not necessarily has to be the same as the interaction in a single particle theory. It is the essence of a two particle theory to take additional correlations into account. HF-theory for instance neglects the correlation between particles of opposite spin. This can be seen by the diagrammatical representation of the self-energy in HF-theory, where the exchange-interaction part does not contribute to the self-energy. The only contribution to the HF-self-energy comes from the direct Coulomb-term, which describes the interaction of an electron with an effective field caused by the other particles in the system. The contribution coming from the exchange-interaction, however, is taken into account in ladder approximation as can be seen from (9). Diagrammatically spoken we did nothing else than another renormalization in order to be able to use SDA-theory. The broken lines in Fig. 2 now has to be imagined as broken double lines indicating an effective interaction in the vertex.

The effective potential as a function of the bare Hubbard- U can be seen in Fig. 4 for the *fcc*-lattice at $T = 0K$ and three different band-occupations. Since the effective potential seems to saturate for larger values of U we restricted ourselves to U -values up to 7eV.

The SDA-QDOS is mainly given by two weighted δ -like peaks. This two-peak structure is conserved in our

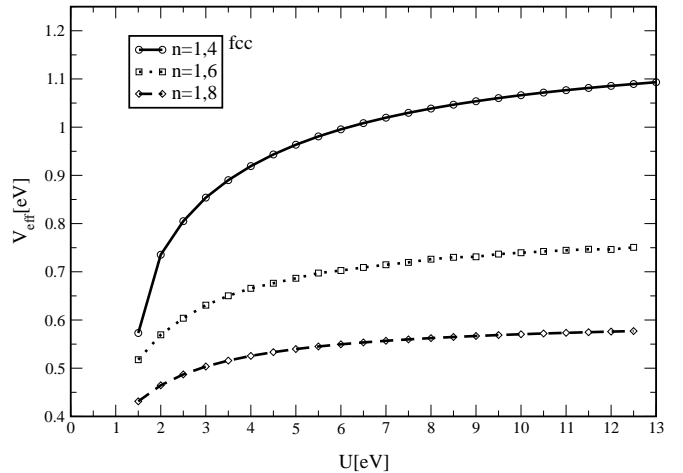


FIG. 4: $V_{eff} = f(U)$ for band occupations $n = 1.4$, $n = 1.6$, $n = 1.8$ at $T = 0K$

MRPA-method. This can be seen from Fig.5, where $\text{Re} \hat{\chi}_{\mathbf{q}}^{+-(\text{MRPA})}(E_n)$ and $\text{Re}(1 - V_{eff} \Lambda_{\uparrow\downarrow}(\mathbf{q}, E_n))$ are plotted for $\mathbf{q} = \mathbf{0}$ and $\mathbf{q} = \pi$ as a function of Energy. The

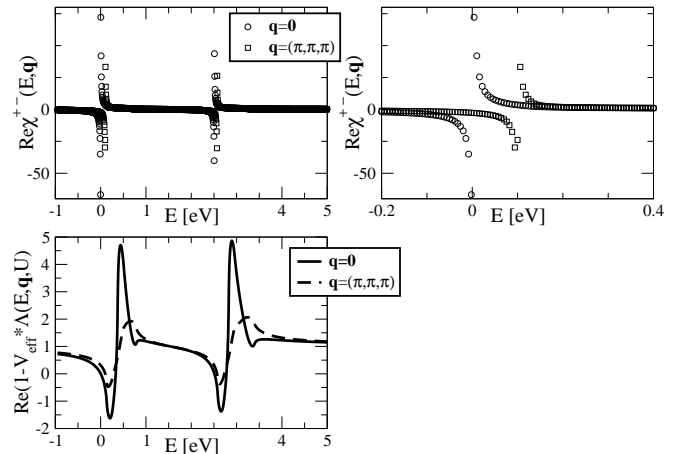


FIG. 5: Upper graphs: $\text{Re} \hat{\chi}_{\mathbf{q}}^{+-(\text{MRPA})}(E_n)$ for $\mathbf{q} = \mathbf{0}$ and $\mathbf{q} = (\pi, \pi, \pi)$, the two-peak structure of the two-particle spectral density is clearly visible in the upper left graph; the lower graph shows $\text{Re}(1 - V_{eff} \Lambda_{\uparrow\downarrow}(\mathbf{q}, E_n))$ to indicate the poles of (10)

effect of the SDA is that the upper set of \mathbf{q} -dependent curves, i.e. the one shifted by $\sim U$ as a result of the SDA-input, shows a dispersion too. This set could be identified as optical modes which are not present in RPA-theory. Calculations for the real substances Fe²³ and Ni²², however, indicate that a separation between acoustical and optical modes about $\sim U$ is one order of magnitude to large. That is why we only did look at the low lying excitation mode.

V. RESULTS AND DISCUSSION

In this section we present the results of MRPA and RPA. The latter one we used as the established ‘test’ theory for our purposes.

In MRPA we restricted ourselves to the *fcc*-lattice since an asymmetric quasi particle density of states (Q-DOS) supports the tendency towards a ferromagnetic alignment of the spins in the Hubbard-model²⁶.

Figure 6 shows isotropic spin wave dispersions as a function of U for the *fcc*-lattice in MRPA. The dispersion curves were computed along different directions of high symmetry in the First-Brillouin-Zone (FBZ). This isotropy for the *fcc*-lattice is in agreement with results observed using Gutzwiller-ansatz¹.

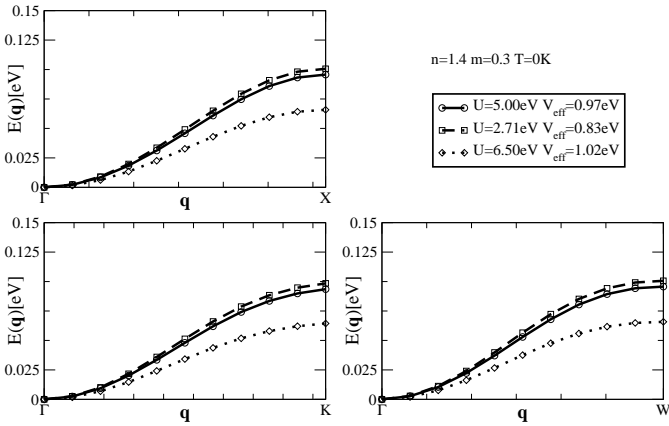


FIG. 6: Magnon dispersion in MRPA along different high symmetry directions of the FBZ for the *fcc*-lattice, parameter: $U = 2.71\text{eV}; 5.00\text{eV}; 6.50\text{eV}$ at fixed band occupation $n = 1.4$, $T = 0\text{K}$, see the bordered box for values of V_{eff}

Figure 6 also shows the behaviour of the stiffness D in dependency of the correlation parameter U . For increasing values of U the magnon energy at the edge of the FBZ weakens or in other words D decreases with increasing U . In Fig. 7 $E(\mathbf{q} = (\pi, \pi, \pi)) = f(U)$ is plotted for RPA and MRPA for fixed band occupations in either case. We see that in RPA theory the magnon energy at the edge of the FBZ continuously increases up to a maximum and afterwards decreases with higher values of U . In MRPA the magnon energy at the edge of the FBZ decreases continuously with increasing U . This is in contrast to a statement given by Bünnemann et.al.⁸ where the authors found the opposite behaviour using (multiband) RPA namely increasing D with increasing U . The behaviour of decreasing D with increasing U on the other hand was observed by Bünnemann et.al.¹ using their recently developed multiband Gutzwiller-ansatz.

We rather think that the decreasing D with increasing U -behaviour is an intrinsic feature of the Hubbard-model.

To us the most surprising result is that using RPA we could compute a qualitatively rather new $T_C(n)$ -phase

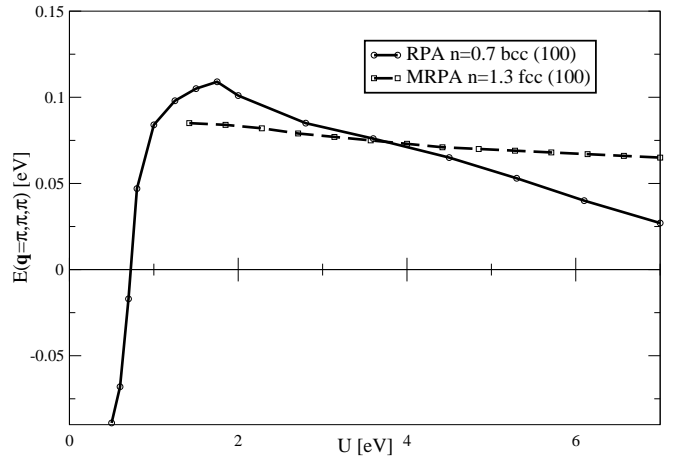


FIG. 7: Behaviour of magnon energies at the edge of the FBZ as a function of U for RPA and MRPA at $T = 0\text{K}$, qualitatively similar behaviour for larger U -values in both theories

diagram which is to see in Fig. 8.

Figure 8 compares HF-phase diagrams with the corresponding phases where the spin wave mode, indicated by subscript SW, exists for three interaction strengths U for the *bcc*-lattice. One example shows a similar behaviour for the *fcc*-lattice.

Numerically we distinguished the SW phase by looking at the stiffness or the magnon energy at the edge of the FBZ respectively. This means that whenever the stiffness D becomes negative the ferromagnetic state breaks down.

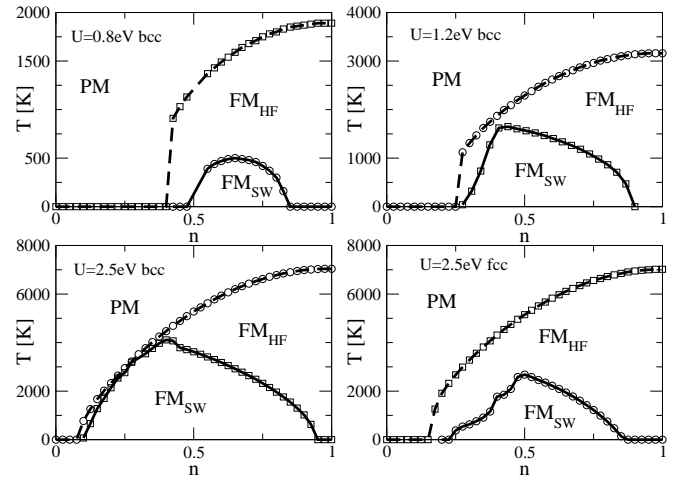


FIG. 8: RPA: $T_C(n)$ -phase diagrams, the upper curves are $T_C(n)$ -phase diagrams computed with single-particle HF-theory denoted by subscript HF, in each case the lower curves indicate the phases where spin waves are excited denoted by subscript SW

The dramatic influence of the spin wave mode on the stability of the ferromagnetic phase is obvious from Fig. 8. Since Stoner-theory overestimates the possibility of ferromagnetic ordering in the Hubbard-model the lack

of the single particle theory is compensated by the corresponding two-particle theory and even results in new Curie-temperatures.

This feature of the RPA is also described for the case of Neel-temperatures³.

In the modified theory MRPA the influence of the collective mode on the shape of the $T_C(n)$ -phase diagram can be seen from Fig. 9. The resulting phase diagram again is physically understandable. The excitation of

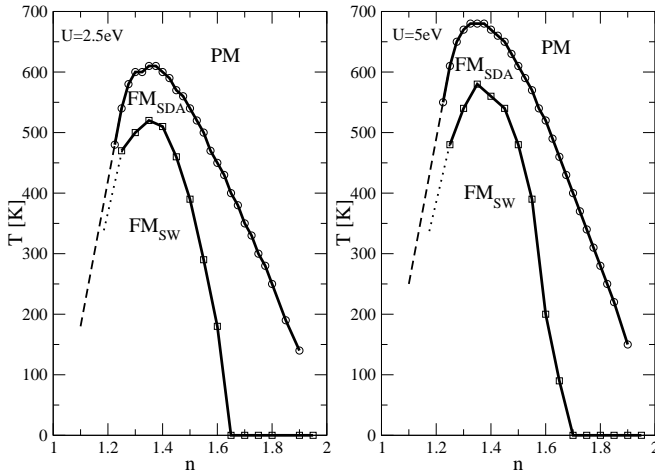


FIG. 9: MRPA: Comparison of single and two-particle phase diagram, in each case the upper curve is the $T_C(n)$ -curve from SDA-theory denoted by subscript SDA, the lower curves are the ‘collective’ phases denoted by subscript SW, fcc-lattice

spin waves reduces Curie-temperatures and the region of band occupation but the qualitative shape more or less stays the same as in the single particle theory.

The ferromagnetic phase for both theories in general is reduced due to weakening of the spin wave dispersion close to half filling and the temperatur driven increased magnon excitation. From figure 9 can be seen that the T_C -curves have their peaks for $n \sim 1.4$. This feature is due to the fact that the bandoccupation that favours a ferromagnetic alignment of the spins in the SDA-approach is mainly given by the lattice-structure. For the fcc-lattice the favourable bandoccupation is $n > 1$ and for $n \sim 1.4$ the ferromagnetic groundstate is almost saturated. The concrete value for T_C is mainly given as a function of the correlation strength U .

Comparison with $T_C(n)$ -phase diagrams of different single particle approximations²⁸ including SDA and the numerically exact Quantum-Monte-Carlo-Simulation¹⁹ demonstrate that besides Curie-temperatures the region of band occupation where ferromagnetism exists is reduced. This indicates that our ‘collective’-phase diagrams are much more reliable then the ones computed using the corresponding single particle theories.

VI. SUMMARY AND OUTLOOK

In the present paper we computed spin wave dispersions and $T_C(n)$ -phase diagrams using standard RPA theory and a modified theory where a reliable approximation for a single particle Green function is used as an input for the two particle Green function. Although we did not follow a stringent mathematical procedure for our MRPA as described exemplary for the case of RPA in²⁵ we were able to show that our results using the modified theory MRPA gives physically reasonable results. These results are comparable to results which we get using standard RPA and to results of a different method namely the Gutzwiller-ansatz as described in¹. Although RPA is a widely used standard technique^{2,3,4,5,6,7} to our knowledge a ‘complete’ $T_C(n)$ -phase diagram was not published before.

Our aim was to get a deeper insight into the phenomenon of collective excitations in a model bandferromagnet. To a ‘first’ approximation our results show that just counting on a single particle theory in order to describe the problem of collective magnetism is not informative enough. Collective excitations strongly influence the stability of a ferromagnetic state and one might use ‘collective’-phase diagrams as tests for single particle theories.

If one wanted to improve the whole theory one had to find an approximation for the vertex function better, i.e. more informative, than ladder approximation and an approximation for the single particle selfenergy at the same theoretical level. Parquet-Ansatz in connection with Coherent-Potential-Approximation CPA as described for the electrical conductivity in the Anderson model²⁷ might be a good starting point. A CPA-type approximation be able to hold for ferromagnetism in this respect is the Modified-Alloy-Analogy (MAA)²⁹ which already yields an improved phase-diagram compared to the SDA-approach²⁸.

* rumsch@physik.hu-berlin.de

¹ J. Büinemann, xxx.lanl.gov, arXiv:cond-mat/0005154, 09.05.2000

² T. Okabe, Phys. Rev. B **57**, 57 (1997)

³ A. Singh, xxx.lanl.gov, arXiv:cond-mat/9802047

⁴ F. Aryasetiawan, K. Karlson, Phys. Rev. B **60**, 7419 (1999)

⁵ K. Karlson, F. Aryasetiawan, J. Phys.:Condens. Matter **12** 7617 (2000)

⁶ S. Schäfer, P. Schuck, arXiv:cond-mat/9804011

Phys. Rev. B **59**, 1712 (1999)

⁷ L. H. M. Barbosa, R. B. Muniz, A. T. Costa, Jr., J. Mathon, Phys. Rev. B textbf{63} 174401 (2001)

⁸ J. Büinemann, F. Gebhard, xxx.lanl.gov, arXiv:cond-mat/0107050

⁹ J. Hubbard, Proc. Roy. Soc. London Ser. A, 238 (1963)

¹⁰ M. C. Gutzwiller, Phys. Rev. Lett. **10**, 159 (1963)

¹¹ J. Kanamori, Prog. Theor. Phys. (Kyoto) **10**, 275 (1963)

¹² E. H. Lieb, F. Y. Wu, Phys. Rev. Lett. **20** 1445 (1968)

¹³ N. D. Mermin, H. Wagner, Phys. Rev. Lett. **17** 1133 (1966)

¹⁴ W. Nolting, Grundkurs: Theoretische Physik Bd.7, Vierteilchentheorie (Springer-Verlag, 5. Auflage, 2002)

¹⁵ W. Nolting, Z.Physik **255**, 25 (1972)

¹⁶ A. B. Brooks, R. V. Lange, Phys. Rev. Letters **157**, 295 (1967)

¹⁷ T. Matsubara, Prog. Theor. Phys. **14**, 351 (1955)

¹⁸ R. Jelitto, J. Phys. Chem. Solids **30**, 609 (1969)

¹⁹ M. Ulmke: Eur. Phys. J. B **1**, 301 (1998)

²⁰ D. M. Edwards Proc. Roy. Soc. **269**, 338 (1962)

²¹ R. V. Lange, Phys. Rev. Letters **146**, 301 (1965)

²² J. F. Cooke and J. A. Blackman and T. Morgan, Phys. Rev. Lett **54**, 718 (1985)

²³ J. F. Cooke and J. A. Blackman and T. Morgan, Phys. Rev. Lett **55**, 2814 (1985)

²⁴ W. Nolting, Z.Phys.B **80**, 73 (1990)

²⁵ G. Baym, L. P. Kadanoff, Phys. Rev. **124**, 287 (1961)

²⁶ R. Arita, S. Onoda, K. Kuroki, H. Aoki, J. Phys. Soc. Japan **69**, 785 (2000)

²⁷ V. Janis, xxx.lanl.gov, arXiv:con-mat/0010044

²⁸ W. Nolting et al. in Band-Ferromagnetism, Eds. K. Baberschke, M. Donath, W. Nolting (Springer-Berlin, LNP580, 2001)

²⁹ M. Potthoff, T. Herrmann, T. Wegner, W. Nolting, phys. stat. sol.(b) **210**, 199 (1998)